

Influence of magnetite stoichiometry on the binding of emerging organic contaminants

Wei Cheng, Rémi Marsac, Khalil Hanna

► **To cite this version:**

Wei Cheng, Rémi Marsac, Khalil Hanna. Influence of magnetite stoichiometry on the binding of emerging organic contaminants. *Environmental Science & Technology*, American Chemical Society, 2018, 52 (2), pp.467-473. 10.1021/acs.est.7b04849 . insu-01662350

HAL Id: insu-01662350

<https://hal-insu.archives-ouvertes.fr/insu-01662350>

Submitted on 13 Dec 2017

HAL is a multi-disciplinary open access archive for the deposit and dissemination of scientific research documents, whether they are published or not. The documents may come from teaching and research institutions in France or abroad, or from public or private research centers.

L'archive ouverte pluridisciplinaire **HAL**, est destinée au dépôt et à la diffusion de documents scientifiques de niveau recherche, publiés ou non, émanant des établissements d'enseignement et de recherche français ou étrangers, des laboratoires publics ou privés.

Influence of magnetite stoichiometry on the binding of emerging organic contaminants

Wei Cheng, Rémi Marsac, and Khalil Hanna

Environ. Sci. Technol., **Just Accepted Manuscript** • DOI: 10.1021/acs.est.7b04849 • Publication Date (Web): 07 Dec 2017

Downloaded from <http://pubs.acs.org> on December 13, 2017

Just Accepted

“Just Accepted” manuscripts have been peer-reviewed and accepted for publication. They are posted online prior to technical editing, formatting for publication and author proofing. The American Chemical Society provides “Just Accepted” as a free service to the research community to expedite the dissemination of scientific material as soon as possible after acceptance. “Just Accepted” manuscripts appear in full in PDF format accompanied by an HTML abstract. “Just Accepted” manuscripts have been fully peer reviewed, but should not be considered the official version of record. They are accessible to all readers and citable by the Digital Object Identifier (DOI®). “Just Accepted” is an optional service offered to authors. Therefore, the “Just Accepted” Web site may not include all articles that will be published in the journal. After a manuscript is technically edited and formatted, it will be removed from the “Just Accepted” Web site and published as an ASAP article. Note that technical editing may introduce minor changes to the manuscript text and/or graphics which could affect content, and all legal disclaimers and ethical guidelines that apply to the journal pertain. ACS cannot be held responsible for errors or consequences arising from the use of information contained in these “Just Accepted” manuscripts.

1 **Influence of magnetite stoichiometry on the binding of emerging**
2 **organic contaminants**

3

4 Wei Cheng^a, Rémi Marsac^{a,b}, Khalil Hanna^{*a}

5

6 ^aÉcole Nationale Supérieure de Chimie de Rennes, UMR CNRS 6226, 11 Allée de Beaulieu,
7 35708 Rennes Cedex 7, France8 ^bGéosciences Rennes, UMR 6118 CNRS – Université Rennes 1, Campus de Beaulieu, 35042
9 Rennes Cedex, France

10 *Corresponding author: Tel.: +33 2 23 23 80 27; fax: +33 2 23 23 81 20.

11 E-mail address: khalil.hanna@ensc-rennes.fr (K. Hanna)

12

13 A revised manuscript for ES&T

14 *December 2017*

15

16

17

18 **Abstract**

19 While the magnetite stoichiometry (*i.e.* Fe(II)/Fe(III) ratio) has been extensively studied for
20 the reductive transformation of chlorinated or nitroaromatic compounds, no work exists
21 examining the influence of stoichiometry of magnetite on its binding properties. This study,
22 for the first time, demonstrates that the stoichiometry strongly affects the capacity of
23 magnetite to bind not only quinolone antibiotics such as nalidixic acid (NA) and Flumequine
24 (FLU), but also salicylic acid (SA), natural organic matter (humic acid, HA) and dissolved
25 silicates. Fe(II)-amendment of non-stoichiometric magnetite (Fe(II)/Fe(III) = 0.40) led to
26 similar sorbed amounts of NA, FLU, SA, silicates or HA as compared to the stoichiometric
27 magnetite (*i.e.* Fe(II)/Fe(III) = 0.50). At any pH between 6 and 10, all magnetites exhibiting
28 similar Fe(II)/Fe(III) ratio in the solid phase showed similar adsorption properties for NA or
29 FLU. This enhancement in binding capability of magnetite for NA is still observed in
30 presence of environmentally relevant ligands (e.g. 10 mg L⁻¹ of HA or 100 μM of silicates).
31 Using surface complexation modeling, it was shown that the NA-magnetite complexation
32 constant does not vary with Fe(II)/Fe(III) between 0.24 and 0.40, but increases by 8 orders of
33 magnitude when Fe(II)/Fe(III) increases from 0.40 to 0.50.

34 I. Introduction

35 Magnetite is an ubiquitous mixed Fe(II)–Fe(III) oxide in soils and sediments, and is very
36 efficient in environmental remediation owing to its reduction capacity.^{1,2} For this reason, the
37 reactivity of magnetite to reduce various organic^{3–7} and inorganic contaminants^{8–11} has been
38 extensively studied. The stoichiometry of the particles (*i.e.* Fe(II)/Fe(III) ratio that can vary
39 from 0 to 0.5) is one of the most important factors in the reduction reaction, and could govern
40 the reactivity of magnetite in natural systems.^{6,10,11} Exposing non-stoichiometric magnetite
41 (*i.e.* low Fe(II)/Fe(III) ratio) to a source of Fe(II) can restore the 0.5 ratio (*i.e.* perfectly
42 stoichiometric magnetite) through oxidation of adsorbed Fe(II), accompanied by reduction of
43 the octahedral Fe(III) in the underlying magnetite to octahedral Fe(II).^{5,6} Therefore,
44 investigations to recharge magnetite surfaces by Fe(II) in order to enhance its reactivity as
45 well as the effect of magnetite stoichiometry on the reduction of contaminants have attracted
46 great attention.^{4–7} However, very little is known about the impact of Fe(II)-recharge on
47 adsorption properties of the magnetite surface. Although the magnetite adsorption capacity
48 was evaluated for different compounds including heavy metals and radionuclides,^{2,12,13}
49 oxyanions^{14,15} and organic ligands,¹⁶ none has attempted to assess the influence of
50 Fe(II)/Fe(III) ratio on the mechanism and extent of binding of these compounds on magnetite
51 surfaces.

52 In this work, we elucidate these effects in different magnetite suspensions containing
53 Nalidixic Acid (NA) or Flumequine (FLU) (see their structures and speciation in Fig. S1).
54 Because of their growing use in human and veterinary medicine and continuous release into
55 the environment, quinolone antibiotics such as NA and FLU have been detected in surface
56 waters, groundwaters and sediments at concentrations levels ranging from ng L⁻¹ to µg L⁻¹.^{17–}
57 ¹⁹ As the mobility of these compounds in the environment can be strongly affected by
58 interactions with surfaces of soil and sediment mineral particles^{18–19}, a thorough

59 understanding of their sorption behavior is essential. Magnetite and more generally iron
60 (oxy)(hydr)oxides represent important reactive surfaces towards organic ligands in soils and
61 sediments.

62 Here, we examined both ligand adsorption and Fe(II) dissolution as a function of pH for
63 magnetites exhibiting different Fe(II)/Fe(III) ratio, prepared as such, or through Fe(II)
64 recharge of non-stoichiometric magnetite suspensions. The binding capability of magnetite
65 with respect to Fe(II)/Fe(III) ratio was also examined in presence of naturally occurring
66 ligands (e.g. salicylic acid (SA), silicates and humic acid (HA)). Implication of ternary surface
67 complexation (i.e. surface-metal-ligand complex) in enhancement in ligand adsorption was
68 assessed by investigating the impact of other divalent cations (Mn(II), Ni(II)) on NA
69 adsorption, where metal binding with no electron transfer is supposed to occur on magnetite.
70 We then used surface complexation modeling to describe the observed behavior, and to gain
71 further insights into the mechanisms responsible for enhancing ligand sorption upon Fe(II)-
72 recharge. The present work notably revealed a considerable impact of the magnetite
73 stoichiometry on the sorption capability of magnetite surfaces.

74

75 **II. Experimental**

76 **Chemicals.** If not mentioned, chemicals (all pro analytical quality or better) were obtained
77 from Sigma Aldrich. Leonardite Humic Acid standard (LHA) was purchased from the
78 International Humic Substances Society (IHSS). Solutions were prepared with ultrapure
79 “MilliQ” water (specific resistivity, $18.2 \text{ M}\Omega \text{ cm}^{-1}$) purged with N_2 for 4 h. Magnetite (ideal
80 formula: Fe_3O_4) was synthesized applying a procedure involving a room temperature aqueous
81 precipitation method in an anaerobic chamber (JACOMEX). A 0.3 M HCl solution containing
82 a $\text{FeCl}_2:\text{FeCl}_3$ 1:2 molar ratio was introduced into an N_2 -sparged 25% w/v ammonium
83 (NH_4OH) solution, with continuous stirring at 1400 rpm, leading to instantaneous

84 precipitation of magnetite particles. Because washing steps can lead to the loss of Fe(II),⁶ no
85 washing step was applied to obtain the stoichiometric magnetite (M0.50; the number refers to
86 Fe(II)/Fe(III) ratio). The solid concentration was 25 g L⁻¹ (5g in 200 mL) and the pH was 8.3.
87 Other magnetites, Fe(II)-depleted, were obtained from M0.50. By applying one washing step
88 to a fraction of M0.50 suspension with N₂-purged ultrapure water and then centrifuged for 5
89 min at 4000 rpm, M0.44 was obtained. By applying three washing steps to M0.50, M0.40 or
90 M0.42 can be obtained. By exposing the M0.50 during 24h to a known amount of H₂O₂
91 (following the procedure of Gorski et al.⁶), M0.42 (denoted as M0.42-H₂O₂) and M0.33 were
92 obtained. By exposing the M0.50 during 24h to ambient air, M0.24 was obtained.

93 **Characterization of magnetite particles.** The mineral identify was confirmed by X-ray
94 diffraction (see XRD pattern in Fig. S2). According to TEM micrographs (Fig. S2), the
95 synthetic magnetite particles are 10 to 15 nm in diameter (12.5 nm on average). Similar XRD
96 patterns were found for the different magnetites investigated here, and no notable influence of
97 the stoichiometry of the particles on particle size was observed. Accordingly, B.E.T. surface
98 area did not significantly differ between the magnetites used in this study ($89 \pm 4 \text{ m}^2 \text{ g}^{-1}$).
99 Using the assumption that all magnetite particles are spherical in shape (density = $5.15 \times 10^6 \text{ g}$
100 m^{-3})¹, TEM surface area was determined to be $93 \text{ m}^2 \text{ g}^{-1}$, close to the BET one.

101 An aliquot of each magnetite suspension was taken and digested in N₂-sparged 5 M HCl
102 inside the glovebox overnight with shaking. Dissolved Fe(II) and Fe(III) concentrations were
103 then determined using the phenanthroline method.²⁰ This bulk Fe(II) content was found very
104 close to that determined by acid digestion on the filtered solid, as previously reported.^{5,6} The
105 amount of magnetite bound-Fe(II) ($[\text{Fe(II)}]_{\text{bound}} = [\text{Fe(II)}]_{\text{tot}} - [\text{Fe(II)}]_{\text{aq}}$) was used to calculate
106 the effective Fe(II)/Fe(III) ratio (denoted as $(\text{Fe(II)/Fe(III)})_{\text{bound}}$) in magnetite which was
107 shown to vary with pH (see results and discussion section). $[\text{Fe(II)}]_{\text{tot}}$ is the total concentration

108 of Fe(II) in the suspension (solid + solution) and $[\text{Fe(II)}]_{\text{aq}}$ is the dissolved concentration of
109 Fe(II), measured after filtration (0.2 μm , Whatman) of the magnetite suspension.

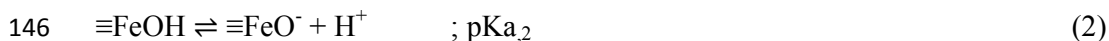
110 **Adsorption experiments.** Adsorption batch experiments were carried out in 15 mL
111 polypropylene tubes under anaerobic conditions (glovebox). NaCl concentration was set to 10
112 mM for all experiments. The effect of dissolved Fe(II) on NA or FLU adsorption to magnetite
113 was investigated by adding small amounts of 100 mM FeCl_2 solution (dissolved in 0.1 M
114 HCl). pH was adjusted using 0.1 M NaOH/HCl solutions. After 24h reaction time, an aliquot
115 was taken and filtered (0.2 μm , Whatman) for high performance liquid chromatography
116 analysis with UV-vis detection (HPLC-UV) and dissolved Fe(II) analysis by the
117 phenanthroline method. Aqueous concentrations of NA or FLU were determined using HPLC
118 (Waters 600 Controller) equipped with a reversed-phase C18 column (250 mm \times 4.6 mm i.d., 5
119 μm) and a UV-vis detector (Waters 2489). The mobile phase was mixture of
120 acetonitrile/water (60/40 v/v) contained 0.1% formic acid. The flow rate was set at 1 ml min^{-1}
121 in isocratic mode. The UV detector was set to 258 nm for NA and 246 nm for FLU.

122 Note that kinetic experiments at pH = 8.5 revealed that (i) NA binding to magnetite
123 (M0.50 or M0.42) and Fe(II) uptake by M0.42 occurred within less than 5 minutes and (ii) the
124 order of adding chemicals (i.e. addition of NA to 24h pre-equilibrated M0.42 with Fe(II) or
125 addition of Fe(II) to 24h pre-equilibrated M0.42 with NA) had no impact on the binding
126 behavior (See Fig. S3). NA adsorption isotherms on M0.50 and M0.42 were also investigated
127 at pH = 7 ($20 \leq [\text{NA}] \leq 300 \mu\text{M}$).

128 The same procedure was applied to test the effect of Mn(II) and Ni(II) on NA adsorption to
129 M0.40. Dissolved Mn(II) and Ni(II) concentrations were determined by Atomic absorption
130 spectroscopy (AAS, Shimadzu). The effect of 10 mg L^{-1} HA or 100 μM silicates on the
131 adsorption of 20 μM NA to magnetite was also investigated, applying the same procedure.
132 HA concentrations in solution were monitored using an organic carbon analyzer (Shimadzu

133 TOC-VCSH). SA concentration was determined using UV-Visible spectrophotometer at 297
134 nm. Silicates concentrations were determined by the molybdenum-blue colorimetric method.²¹
135 **Surface complexation modeling.** The geochemical speciation code PHREEQC (version 2)²²
136 and the “minteq” database provided with this code were used. At infinite dilution, the pK_a of
137 NA and FLU equal 6.19 and 6.31, respectively, and the logarithm of the formation constant of
138 NA-Fe⁺_(aq) and FLU-Fe⁺_(aq) equal 3.99 and 4.23, respectively ; as calculated from reported
139 conditional constant values and the Davies equation.^{23,24} The surface complexation models
140 developed by Jolsterå et al.²⁵ for magnetite and maghemite were used to predict NA and FLU
141 adsorption to magnetite with different stoichiometry. Maghemite γ -Fe^{III}₂O₃ is considered as
142 an extreme example of a non-stoichiometric magnetite (Fe^{II}₁Fe^{III}₂O₄), with only Fe^{III} in both
143 tetrahedral and octahedral sites¹.

144 Surface site protonation is formulated as follows (2-pKa approach):



147 Charge-potential relationship is described according to the constant capacitance model
148 (CCM). Model parameters for magnetite and maghemite are reported in Table S1. The CCM
149 is not implemented in PHREEQC, but it can be used via a three plane model (TPM; available
150 in PHREEQC), in which one capacitor and the diffuse layer are suppressed, following the
151 procedure detailed in Marsac et al.²⁶.

152

153 **III. Results and discussion**

154 **Binding capacity vs magnetite stoichiometry.** Nalidixic acid (NA) adsorption to four
155 magnetites exhibiting different Fe(II)/Fe(III) ratio (0.40, 0.42, 0.44 and 0.50) showed that NA
156 adsorption was strongly related to the stoichiometry of the particles (*i.e.* Fe(II)/Fe(III) ratio
157 vary from 0.40 for non-stoichiometric magnetite, to 0.50 for stoichiometric magnetite; Fig.

158 1a). NA adsorption to M0.40 decreased with increasing pH, as typically encountered for
159 anionic ligands, and became negligible for $\text{pH} > 7.5$. Indeed, adsorption of anionic ligands to
160 mineral oxides is typically greatest under acidic to circumneutral pH, and lowest under
161 alkaline conditions, with maximum adsorption generally observed at a pH near the pK_a (i.e.
162 6.19 for NA).²⁷⁻³¹ At higher stoichiometry (0.42, 0.44 or 0.50), pH dependence of NA
163 sorption was significantly altered. NA adsorption increased from pH 6 to $7 < \text{pH} < 8$ and then
164 decreased with increasing pH, thereby shifting the maximum NA adsorption to larger pH
165 values than the pK_a . Note that adsorption of NA to M0.42 prepared either by washing or
166 oxidizing (H_2O_2) of M0.50 was similar. The data are merged in Fig. 1a (see Fig. S4 for more
167 details).

168 Fe(II)-amendment of non-stoichiometric magnetite (M0.40 and M0.42) led also to an
169 enhancement in NA adsorption (Fig. 1a). Indeed, the pH-adsorption curve of NA shifted to
170 larger pH values with increasing added amounts of dissolved Fe(II), a result suggesting that
171 NA binding was closely related to the Fe(II) content or Fe(II)/Fe(III) ratio in magnetite. The
172 Fe(II) recharge of non-stoichiometric magnetite provided the same adsorption capability as
173 for the corresponding magnetite with higher stoichiometry on the whole pH-range
174 investigated (i.e. Fe(II)/Fe(III) = 0.42 for M0.40 + 100 μM Fe(II) and M0.42 ; Fe(II)/Fe(III) =
175 0.44 for M0.40 + 200 μM Fe(II) and M0.44 ; Fe(II)/Fe(III) = 0.50 for M0.40 + 500 μM Fe(II),
176 M0.42 + 400 μM Fe(II) and M0.50).

177 Because of Fe(II) dissolution, the amount of bound-Fe(II) in magnetite can vary
178 depending on pH, which may affect the NA adsorption. Indeed, $[\text{Fe(II)}]_{\text{aq}}$ increased with
179 decreasing pH (no dissolved Fe(III) was found), due to the H^+ promoted dissolution of
180 magnetite,^{32,33} but also with magnetite stoichiometry (i.e. $\text{M0.40} < \text{M0.44} < \text{M0.50}$) (Figure
181 1b). Exposing a non-stoichiometric magnetite (M0.40) to 200 or 500 μM Fe(II) led to similar
182 Fe(II) aqueous concentration as those measured with M0.44 or M0.50, respectively. Note that

183 only up to ~10% of magnetite could dissolve in our experiments (*e.g.* for M0.50 at the lowest
184 pH investigated, *i.e.* 6). Therefore, the effect of magnetite dissolution on NA adsorption can
185 be neglected.

186 As expected, $(\text{Fe(II)/Fe(III)})_{\text{bound}}$ increased with Fe(II)-recharge of non-stoichiometric
187 magnetite and pH (Figure 1c). Variation in $(\text{Fe(II)/Fe(III)})_{\text{bound}}$ appeared fully consistent with
188 the magnetite ability to bind NA. For instance, all magnetites exhibiting similar
189 $(\text{Fe(II)/Fe(III)})_{\text{bound}}$ values showed similar NA sorbed amounts whatever the investigated pH,
190 though the dissolved Fe(II) amounts are different (especially at low pH values < 7.5) (Fig.
191 1b). For instance, M0.50 shows the same binding capability for NA as for the corresponding
192 Fe(II)-amended magnetite (*i.e.* M0.40 + 500 μM Fe(II) and M0.42 + 400 μM Fe(II)), and
193 therefore similar surface properties with respect to NA adsorption. This is also true for M0.40
194 + 200 μM Fe(II) *vs* M0.44, and further illustrated in Fig. S5, where variations of NA sorbed
195 amounts at pH 7.7 as a function of $(\text{Fe(II)/Fe(III)})_{\text{bound}}$ followed the same trend for both
196 stoichiometric magnetite (M0.5) and Fe(II)-amended non-stoichiometric magnetites (M0.40
197 and M0.44). Likewise, enhancement in Flumequine (FLU) adsorption was observed with
198 increasing amounts of added Fe(II) to M0.40 or $(\text{Fe(II)/Fe(III)})_{\text{bound}}$ (Fig. S6). Desorption tests
199 were conducted by adjusting pH to 11 after the system has reached equilibrium and then
200 stirred for around 2 h. Mass balance showed that NA or FLU was removed only by adsorption
201 and that transformation by, for example, reduction, did not occur under the experimental
202 conditions of this study.

203 Formation of ternary surface complexes (*i.e.* surface-metal-ligand complex) generally
204 entails more ligand adsorption when complexing cation concentration increases³⁴, which
205 might explain the enhancement in NA or FLU binding to magnetite. To test this hypothesis,
206 impacts of presence of two divalent cations (Mn(II) and Ni(II)) on NA adsorption to M0.40
207 were investigated and compared with that of Fe(II). Because the redox potential of the

208 $\text{Mn}^{\text{II}}/\text{MnO}_{2(\text{s})}$ couple at $\text{pH} = 7$ is much larger than that of $\text{Fe}^{\text{II}}/\text{Fe}_3\text{O}_{4(\text{s})}$, Mn(II) oxidation by
209 magnetite is not expected.³⁵ According to the Irving-Williams series,³⁶ cation adsorption
210 data³⁵ and aqueous complexation with NA,^{23,37} ternary surface complexation of Mn(II), Fe(II)
211 and Ni(II) with NA on magnetite are supposed to follow the order: $\text{Mn}(\text{II}) < \text{Fe}(\text{II}) < \text{Ni}(\text{II})$ ³⁴
212 (assuming that no electron transfer occurs between Fe(II) and the solid). This ranking is,
213 however, observed neither for metal uptake nor for NA adsorption to M0.40 (Fig. 2). Indeed,
214 more Fe(II) uptake than Ni(II) is achieved (Fig. 2a), whereas maximum NA adsorption was
215 obtained at $\text{pH} \approx 7.5$ for Fe(II) and $\text{pH} \approx 8.5$ for Mn(II) and Ni(II). This observation is also
216 confirmed at higher metal concentration (e.g. $500\mu\text{M}$, Fig. S7), thereby underscoring a
217 different adsorption behavior of NA in presence of Fe(II) with respect to other divalent
218 transition metals.

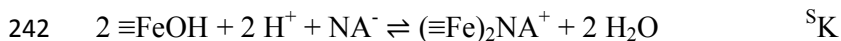
219 Taken together, these findings suggest that the adsorption enhancement for NA is mainly
220 controlled by the $(\text{Fe}(\text{II})/\text{Fe}(\text{III}))_{\text{bound}}$ ratio in magnetite, rather than by NA-Fe(II)
221 complexation in solution at low pH or ternary surface complexation. As a matter of fact, the
222 enhanced binding of ligands to stoichiometric magnetite with respect to non-stoichiometric
223 one may result from the creation of new binding sites upon Fe(II)-recharge, or changes in the
224 intrinsic surface reactivity of amended magnetite.

225

226 **Description of enhancement sorption capacity.** As an attempt to describe the
227 relationship between $(\text{Fe}(\text{II})/\text{Fe}(\text{III}))_{\text{bound}}$ and ligand adsorption, we used a surface
228 complexation modeling approach. The aim of the present modeling exercise was to provide a
229 semi-quantitative evaluation of how much magnetite surface reactivity towards quinolones is
230 affected by its stoichiometry. Because of the possible presence of various types of
231 $\equiv\text{Fe}^{\text{II/III}}\text{O}(\text{H})$ groups at magnetite surfaces, full mechanistic description of binding
232 mechanisms using a complete approach would have required fitting of many parameters, and

233 then generated large errors on simulated phenomena. Therefore, we used the 2-pKa-CCM
234 approach developed by Jolsterå et al.²⁵. Using acid-base titration method, they have calculated
235 site densities of 1.50 nm⁻² and 0.99 nm⁻² for magnetite (91 m² g⁻¹) and maghemite (86 m² g⁻¹),
236 respectively

237 As shown in Figure S8, fitting experimental adsorption isotherms of NA on M0.50 and
238 M0.42 at pH = 7 with Langmuir equation results in a maximum binding capacity of 0.95 and
239 0.71 NA molecule nm⁻², respectively. Previous studies on quinolones binding to iron
240 (hydr)oxides evidenced that one molecule binds to two surface hydroxo groups,^{29,38,39} by
241 involving its carboxylate and its keto-group as following:



243

244 Hence, the maximum binding of NA to magnetites corresponds to 1.90 to 1.42 site nm⁻²,
245 which are relatively close to those determined by Jolsterå et al.²⁵. As the present modeling
246 exercise aimed to determine surface complexation constant (^SK) to each magnetite, we
247 focused only on the pH-edge curve (obtained at low surface coverage) and thus used the same
248 site density for all magnetites (1.50 nm⁻²). Measured total dissolved Fe(II) concentration in
249 solution at the end of each adsorption experiment was used as input parameter to account for
250 ligand-Fe(II) complexation in solution. However, decreasing ligand adsorption with
251 decreasing pH (i.e. at high [Fe(II)]_{aq}) could not be well predicted, further suggesting that
252 effects of variation of (Fe(II)/Fe(III))_{bound} were more important than the ligand-Fe(II) aqueous
253 complexation. Therefore, we only focused on data at high pH values, where
254 (Fe(II)/Fe(III))_{bound} is maximal and constant (see Fig. 1c; e.g. pH > 8 for M0.50, pH > 6.5 for
255 M0.40). As shown in Figure 1a (NA) and Figure S6 (FLU), a relatively good fit to the
256 adsorption data versus pH was found (unsuccessful extrapolations at lower pH are shown as
257 dotted lines in Fig. 1a and S6). When plotting log ^SK for NA versus (Fe(II)/Fe(III))_{bound} (Fig.

258 3), a linear relationship was found ($R^2=0.99$). Data for FLU are also included and show a
259 comparable behavior. Values of $\log {}^S K$ increased by almost 8 orders of magnitude with
260 increasing $(\text{Fe(II)/Fe(III)})_{\text{bound}}$ from 0.40 to 0.50, suggesting that stoichiometric magnetite
261 (Fe(II)-enriched) may have a much stronger affinity for NA or FLU than partially oxidized
262 magnetite (Fe(II)-depleted). Such large variation in $\log {}^S K$ cannot be attributed to potential
263 modification in surface site density that was neglected by using the same site density for all
264 magnetites. As more amount of Fe(II) at the magnetite surface is expected upon Fe(II)
265 recharge, we may suppose that $\equiv\text{Fe}^{\text{II}}\text{O(H)}$ sites are more reactive than $\equiv\text{Fe}^{\text{III}}\text{O(H)}$ for NA or
266 FLU binding.

267 To test the binding capacity of magnetite with lower stoichiometries, we prepared
268 M0.33 and M0.24 (similar to magnetites found in some natural samples^{40,41}), by exposing the
269 M0.50 during 24h to (i) a known amount of H_2O_2 (following the procedure of Gorski et al.⁶)
270 and (ii) ambient air, respectively. Both oxidized magnetites exhibited similar NA adsorption,
271 whereas $[\text{Fe(II)}]_{\text{aq}}$ were found very low (Fig. 1b). For $\text{pH} \leq 7$, more pronounced NA
272 adsorption was observed on M0.33 and M0.24 as compared to M0.40, a result that can be
273 attributed to the complete suppression of dissolved Fe(II) at low pH. Consistently, the best
274 fitting values of ${}^S K$ were found very close for M0.24, M0.33 ($\log {}^S K = 17.7$) and M0.40 (\log
275 ${}^S K = 17.5$). It is worth noting that the calculated surface complexation constant ${}^S K$ remains
276 constant for $0.23 < \text{Fe(II)/Fe(III)}_{\text{bound}} < 0.40$, and then sharply increased after 0.40 (Fig. 2).
277 The existence of a threshold may be related to the surface amount of magnetite bound-Fe(II)
278 required to trigger the enhancement of NA binding with magnetite surfaces.

279 Because non-stoichiometric magnetites may have oxidized magnetite/maghemite-like
280 structure at the outermost surface (oxidation of magnetite particles is supposed to take place
281 from the surface to the core²⁵), NA adsorption to magnetites with $\text{Fe(II)/Fe(III)} \leq 0.42$ was
282 also evaluated using the surface complexation model developed for maghemite (i.e. fully

283 oxidized magnetite). Because of the little variation in site density, surface area and acid-base
284 properties, $\log K$ (for NA and FLU) determined using magnetite model or maghemite model
285 were found very similar (Fig. 4).

286 This modification in binding properties is not specifically limited to NA or FLU
287 molecule, since the adsorption of naturally occurring ligands such as salicylate (1-
288 hydroxybenzoic acid, SA), humic acid (HA) and silicates (Si) was also considerably enhanced
289 by the addition of dissolved Fe(II) to a non-stoichiometric magnetite M0.40 (See Figures S9-
290 S11). Consequently, the stoichiometry of magnetite is not only a key parameter for Fe(II)
291 uptake⁵ and contaminant reduction^{6,10,11} but also for the binding of emerging organic
292 contaminants and naturally occurring ligands. Because emerging contaminants binding to
293 magnetite might be affected by naturally occurring ligands, competitive experiments between
294 NA and HA or Si were conducted. The presence of 100 μM Si decreased NA binding to
295 magnetite due to ligand competition, though the effect of Si on NA adsorption to M0.40 is
296 insignificant (Fig. 4a). However, the impact of 10 mg L^{-1} HA on NA binding implies both
297 competitive (i.e. antagonistic effect) and cooperative (i.e. synergetic effect) mechanisms (Fig.
298 4b). Indeed, at high Fe(II)/Fe(III), HA effectively decreases NA binding whereas, at low
299 Fe(II)/Fe(III), NA binding is enhanced in presence of HA. The latter may arise from
300 intermolecular interactions between HA and NA, as previously observed between NA and
301 other organic compounds at goethite surfaces,^{38,39} and supported by a quinolone-HA binding
302 study.⁴² While further investigations are required to understand the different competitive and
303 cooperative effects, this data further supports that (i) binding properties of magnetite is
304 affected upon Fe(II)-recharge, and (ii) this change towards adsorption of emerging
305 contaminants is still observed in presence of naturally occurring ligands.

306 **Environmental implications.** Magnetites of differential composition and
307 stoichiometry may exist in natural systems depending on the local redox and chemical

308 conditions, particularly in Fe-rich subsurface environments or temporary flooded soils (e.g.
309 wetlands experiencing redox potential fluctuation).^{1,2,38,39} Given its higher solubility and
310 surface area-to-volume ratio, Fe(II) release and/or surface oxidation may occur for the
311 nanosized magnetite, commonly found in environmental systems¹. On the other hand,
312 different kinds of magnetite can be obtained depending on the synthesis method, as reported
313 in water remediation studies using magnetite as sorbent.^{27,31,32} Consequently, the
314 stoichiometry of magnetite and its potential Fe(II)-enrichment or Fe(II)-depletion in reaction
315 medium should be appropriately considered in sorption and reactive transport studies. It is
316 worth noting that the changes in binding properties of magnetite upon Fe(II)-recharge are still
317 observed in presence of natural ligands, emphasizing the importance of the presently
318 evidenced mechanisms in environmentally relevant conditions. Therefore, these findings call
319 for refinements in current day modeling approaches used in the prediction of fate of organic
320 contaminants in Fe-rich subsurface environments or magnetite-based remediation processes.

321

322 **Acknowledgements.** The authors gratefully acknowledge the financial support of this work
323 by ADEME “Agence de l'Environnement et de la Maîtrise de l'Energie” N° of funding
324 decision 1472C0030.

325

326 **Supporting Information Available.** Characterization data of magnetite particles, NA and
327 FLU aqueous speciation versus pH, surface complexation model parameters, additional
328 results for adsorption kinetics and isotherms, impacts of cationic metals, Si and HA on
329 adsorption behavior. This information is available free of charge via the Internet at
330 <http://pubs.acs.org/>.

331

332 **References**

- 333 (1) Maher, B. A.; Taylor, R. M. Formation of ultrafine-grained magnetite in soils. *Nature* **1988**, *336*
334 (6197), 368–370.
- 335 (2) Singer, D. M.; Chatman, S. M.; Ilton, E. S.; Rosso, K. M.; Banfield, J. F.; Waychunas, G. A. U(VI)
336 Sorption and Reduction Kinetics on the Magnetite (111) Surface. *Environ. Sci. Technol.* **2012**,
337 *46* (7), 3821–3830.
- 338 (3) McCormick, M. L.; Adriaens, P. Carbon Tetrachloride Transformation on the Surface of
339 Nanoscale Biogenic Magnetite Particles. *Environ. Sci. Technol.* **2004**, *38* (4), 1045–1053.
- 340 (4) Gregory, K. B.; Larese-Casanova, P.; Parkin, G. F.; Scherer, M. M. Abiotic Transformation of
341 Hexahydro-1,3,5-trinitro-1,3,5-triazine by Fe^{II} Bound to Magnetite. *Environ. Sci. Technol.* **2004**,
342 *38* (5), 1408–1414.
- 343 (5) Gorski, C. A.; Scherer, M. M. Influence of Magnetite Stoichiometry on Fe^{II} Uptake and
344 Nitrobenzene Reduction. *Environ. Sci. Technol.* **2009**, *43* (10), 3675–3680.
- 345 (6) Gorski, C. A.; Nurmi, J. T.; Tratnyek, P. G.; Hofstetter, T. B.; Scherer, M. M. Redox Behavior of
346 Magnetite: Implications for Contaminant Reduction. *Environ. Sci. Technol.* **2010**, *44* (1), 55–60.
- 347 (7) Klausen, J.; Troeber, S. P.; Haderlein, S. B.; Schwarzenbach, R. P. Reduction of Substituted
348 Nitrobenzenes by Fe(II) in Aqueous Mineral Suspensions. *Environ. Sci. Technol.* **1995**, *29* (9),
349 2396–2404.
- 350 (8) Scheinost, A. C.; Charlet, L. Selenite Reduction by Mackinawite, Magnetite and Siderite: XAS
351 Characterization of Nanosized Redox Products. *Environ. Sci. Technol.* **2008**, *42* (6), 1984–1989.
- 352 (9) Missana, T.; Alonso, U.; Scheinost, A. C.; Granizo, N.; García-Gutiérrez, M. Selenite retention
353 by nanocrystalline magnetite: Role of adsorption, reduction and dissolution/co-precipitation
354 processes. *Geochim. Cosmochim. Acta* **2009**, *73* (20), 6205–6217.
- 355 (10) Huber, F.; Schild, D.; Vitova, T.; Rothe, J.; Kirsch, R.; Schäfer, T. U(VI) removal kinetics in
356 presence of synthetic magnetite nanoparticles. *Geochim. Cosmochim. Acta* **2012**, *96*, 154–173.
- 357 (11) Latta, D. E.; Gorski, C. A.; Boyanov, M. I.; O’Loughlin, E. J.; Kemner, K. M.; Scherer, M. M.
358 Influence of Magnetite Stoichiometry on UVI Reduction. *Environ. Sci. Technol.* **2012**, *46* (2),
359 778–786.
- 360 (12) Giraldo, L.; Erto, A.; Moreno-Piraján, J. C. Magnetite nanoparticles for removal of heavy metals
361 from aqueous solutions: synthesis and characterization. *Adsorption* **2013**, *19* (2–4), 465–474.
- 362 (13) Catalette, H.; Dumonceau, J.; Ollar, P. Sorption of cesium, barium and europium on magnetite.
363 *J. Contam. Hydrol.* **1998**, *35* (1–3), 151–159.
- 364 (14) Daou, T. J.; Begin-Colin, S.; Grenèche, J. M.; Thomas, F.; Derory, A.; Bernhardt, P.; Legaré, P.;
365 Pourroy, G. Phosphate Adsorption Properties of Magnetite-Based Nanoparticles. *Chem.*
366 *Mater.* **2007**, *19* (18), 4494–4505.
- 367 (15) Liu, C.-H.; Chuang, Y.-H.; Chen, T.-Y.; Tian, Y.; Li, H.; Wang, M.-K.; Zhang, W. Mechanism of
368 Arsenic Adsorption on Magnetite Nanoparticles from Water: Thermodynamic and
369 Spectroscopic Studies. *Environ. Sci. Technol.* **2015**, *49* (13), 7726–7734.
- 370 (16) Tombác, E.; Tóth, I. Y.; Nesztor, D.; Illés, E.; Hajdú, A.; Szekeres, M.; L.Vékás. Adsorption of
371 organic acids on magnetite nanoparticles, pH-dependent colloidal stability and salt tolerance.
372 *Colloids Surf. Physicochem. Eng. Asp.* **2013**, *435*, 91–96.
- 373 (17) Heberer, T. Occurrence, fate, and removal of pharmaceutical residues in the aquatic
374 environment: a review of recent research data. *Toxicol. Lett.* **2002**, *131* (1–2), 5–17.
- 375 (18) Fatta-Kassinos, D.; Meric, S.; Nikolaou, A. Pharmaceutical residues in environmental waters
376 and wastewater: current state of knowledge and future research. *Anal. Bioanal. Chem.* **2011**,
377 *399* (1), 251–275.
- 378 (19) Gothwal, R.; Shashidhar, T. Antibiotic Pollution in the Environment: A Review. *CLEAN – Soil Air*
379 *Water* **2015**, *43* (4), 479–489.
- 380 (20) Fortune, W. B.; Mellon, M. G. Determination of Iron with o-Phenanthroline: A
381 Spectrophotometric Study. *Ind. Eng. Chem. Anal. Ed.* **1938**, *10* (2), 60–64.

- 382 (21) Mullin, J. B.; Riley, J. P. The colorimetric determination of silicate with special reference to sea
383 and natural waters. *Anal. Chim. Acta* **1955**, *12*, 162–176.
- 384 (22) Parkhurst, D. L.; Appelo, C. A. J. *User's guide to PHREEQC (Version 2) : a computer program for*
385 *speciation, batch-reaction, one-dimensional transport, and inverse geochemical calculations;*
386 *Water-Resources Investigations Report; USGS Numbered Series 99–4259; Water-resources*
387 *Investigation Report 99–4259. USGS, Denver, Colorado., 1999; p (p. 312).*
- 388 (23) Ross, D. L.; Riley, C. M. Aqueous solubilities of some variously substituted quinolone
389 antimicrobials. *Int. J. Pharm.* **1990**, *63* (3), 237–250.
- 390 (24) Vincent, W. R.; Schulman, S. G.; Midgley, J. M.; van Oort, W. J.; Sorel, R. H. A. Prototropic and
391 metal complexation equilibria of nalidixic acid in the physiological pH region. *Int. J. Pharm.*
392 **1981**, *9* (3), 191–198.
- 393 (25) Jolsterå, R.; Gunneriusson, L.; Holmgren, A. Surface complexation modeling of Fe₃O₄–H⁺ and
394 Mg(II) sorption onto maghemite and magnetite. *J. Colloid Interface Sci.* **2012**, *386* (1), 260–
395 267.
- 396 (26) Marsac, R.; Banik, N. L.; Lützenkirchen, J.; Catrouillet, C.; Marquardt, C. M.; Johannesson, K. H.
397 Modeling metal ion-humic substances complexation in highly saline conditions. *Appl.*
398 *Geochem.* **2017**, *79*, 52–64.
- 399 (27) Paul, T.; Liu, J.; Machesky, M. L.; Strathmann, T. J. Adsorption of zwitterionic fluoroquinolone
400 antibacterials to goethite: A charge distribution-multisite complexation model. *J. Colloid*
401 *Interface Sci.* **2014**, *428*, 63–72.
- 402 (28) Usman, M.; Martin, S.; Cimetière, N.; Giraudet, S.; Chatain, V.; Hanna, K. Sorption of nalidixic
403 acid onto micrometric and nanometric magnetites: Experimental study and modeling. *Appl.*
404 *Surf. Sci.* **2014**, *299*, 136–145.
- 405 (29) Marsac, R.; Martin, S.; Boily, J.-F.; Hanna, K. Oxolinic Acid Binding at Goethite and Akaganéite
406 Surfaces: Experimental Study and Modeling. *Environ. Sci. Technol.* **2016**, *50* (2), 660–668.
- 407 (30) Hanna, K.; Boily, J.-F. Sorption of Two Naphthoic Acids to Goethite Surface under Flow
408 through Conditions. *Environ. Sci. Technol.* **2010**, *44* (23), 8863–8869.
- 409 (31) Rusch, B.; Hanna, K.; Humbert, B. Sorption and Transport of Salicylate in a Porous
410 Heterogeneous Medium of Silica Quartz and Goethite. *Environ. Sci. Technol.* **2010**, *44* (7),
411 2447–2453.
- 412 (32) Jolivet, J.-P.; Tronc, E. Interfacial electron transfer in colloidal spinel iron oxide. Conversion of
413 Fe₃O₄-γ-Fe₂O₃ in aqueous medium. *J. Colloid Interface Sci.* **1988**, *125* (2), 688–701.
- 414 (33) White, A. F.; Peterson, M. L.; Hochella, M. F. Electrochemistry and dissolution kinetics of
415 magnetite and ilmenite. *Geochim. Cosmochim. Acta* **1994**, *58* (8), 1859–1875.
- 416 (34) Fein, J. B. The effects of ternary surface complexes on the adsorption of metal cations and
417 organic acids onto mineral surfaces. In: R. Hellmann and S.A. Wood (Editors), *Water-Rock*
418 *Interactions, Ore Deposits, and Environmental Geochemistry: A Tribute to David A. Crerar.*
419 *Geochemical Society, Special Pub. 7*, p. 365–378.
- 420 (35) Stumm, W.; Morgan, J. J. *Aquatic Chemistry: Chemical Equilibria and Rates in Natural Waters,*
421 *3rd ed*, John Wiley & Sons, Inc., New York.; 1996.
- 422 (36) Irving, H.; Williams, R. J. P. The stability of transition-metal complexes. *J. Chem. Soc. Resumed*
423 **1953**, *0* (0), 3192–3210.
- 424 (37) Timmers, K.; Sternglanz, R. Ionization and divalent cation dissociation constants of nalidixic
425 and oxolinic acids. *Bioinorg. Chem.* **1978**, *9* (2), 145–155.
- 426 (38) Xu, J.; Marsac, R.; Wei, C.; Wu, F.; Boily, J.-F.; Hanna, K. Co-binding of Pharmaceutical
427 Compounds at Mineral Surfaces: Mechanistic Modeling of Binding and Cobinding of Nalidixic
428 Acid and Niflumic Acid at Goethite Surfaces. *Environ. Sci. Technol.* **2017**, *51* (20), 11617–
429 11624.
- 430 (39) Xu, J.; Marsac, R.; Costa, D.; Cheng, W.; Wu, F.; Boily, J.-F.; Hanna, K. Co-Binding of
431 Pharmaceutical Compounds at Mineral Surfaces: Molecular Investigations of Dimer Formation
432 at Goethite/Water Interfaces. *Environ. Sci. Technol.* **2017**, *51* (15), 8343–8349.

- 433 (40) Haggstrom, L.; Annersten, H.; Ericsson, T.; Wappling, R.; Karner, W.; Bjarman, S. Magnetic
434 Dipolar and Electric Quadrupolar Effects on Mossbauer-Spectra. *Hyperfine Interact.* **1978**, *5*
435 (3), 201–214.
- 436 (41) Vandenberghe, R. E.; Hus, J. J.; Grave, E. D. Evidence from Mössbauer spectroscopy of neo-
437 formation of magnetite/maghemite in the soils of loess/paleosol sequences in China.
438 *Hyperfine Interact.* **1998**, *117* (1–4), 359–369.
- 439 (42) Aristilde, L.; Sposito, G. Complexes of the antimicrobial ciprofloxacin with soil, peat, and
440 aquatic humic substances. *Environ. Toxicol. Chem.* **2013**, *32* (7), 1467–1478.
- 441

442

443 **Figure captions**

444 **Figure 1.** (a) NA adsorption data versus pH for 50 m² L⁻¹ suspensions of M0.24, M0.33,
445 M0.40, M0.42, M0.44, M0.5 and Fe(II)-amended M0.40 and M0.42 versus pH in a 10 mM
446 NaCl + 20 μM NA solution, after 24h reaction time. Lines correspond to surface
447 complexation modeling results (see text for more details). (b) Final Fe(II) aqueous
448 concentration ([Fe(II)]_{aq}) and (c) calculated (Fe(II)/Fe(III))_{bound} in the corresponding
449 experiments. The same legend is used in (a), (b) and (c). The same color is used for
450 experiments conducted with the same total Fe(II)/Fe(III) ratio.

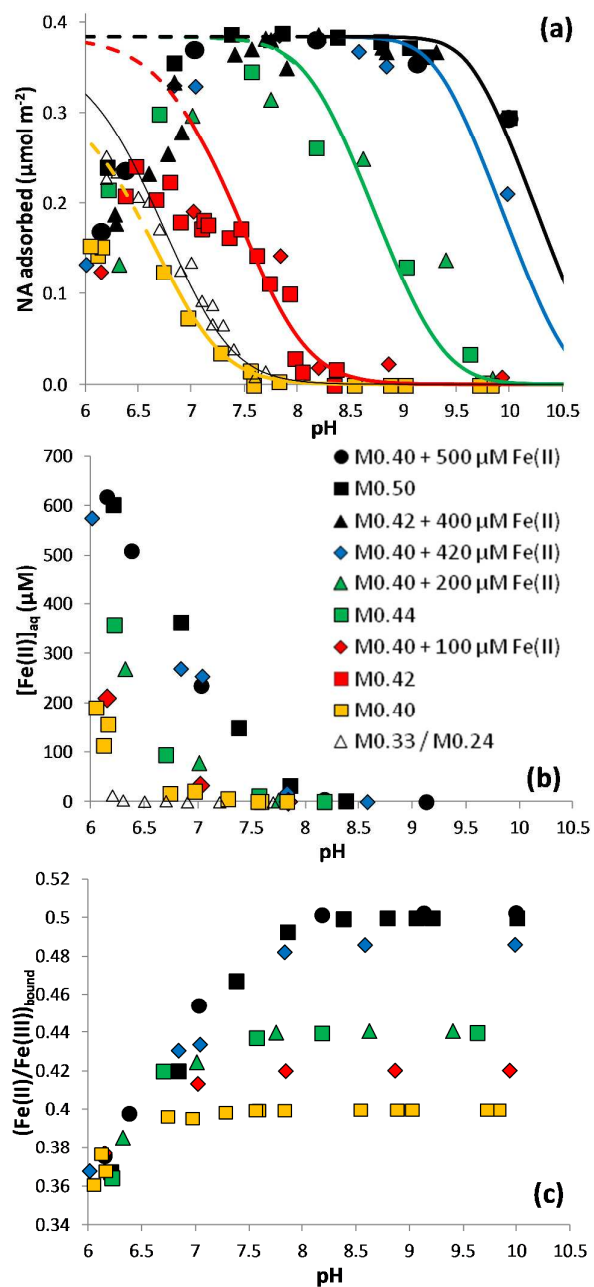
451 **Figure 2.** (a) Uptake data of 200μM Mn(II), Fe(II) or Ni(II) on M0.40 and (b) corresponding
452 NA adsorption data versus pH. Experimental conditions: 50 m² L⁻¹ suspensions of magnetite,
453 10 mM NaCl, 20 μM NA, 200μM Mn(II), Fe(II) or Ni(II), 24h reaction time. Negative values
454 for Fe(II) uptake at low pH are due to magnetite dissolution.

455 **Figure 3.** Logarithm of surface complexation constant (log ^SK, for NA or FLU) versus
456 (Fe(II)/Fe(III))_{bound} determined at pH ≥ 8 (where (Fe(II)/Fe(III))_{bound} is constant). This
457 modeling data was obtained using either a magnetite model (for all data) or maghemite (for
458 Fe(II)/Fe(III) ≤ 0.42).²⁵

459 **Figure 4.** NA adsorption data versus pH for 50 m² L⁻¹ suspensions of M0.40 and Fe(II)-
460 amended M0.40 in a 10 mM NaCl + 20 μM NA solution, after 24h reaction time, in presence
461 of (a) silicates (100 μM) or (b) HA (10 mg L⁻¹). Empty symbols represent the NA adsorption
462 data without Si or HA.

463

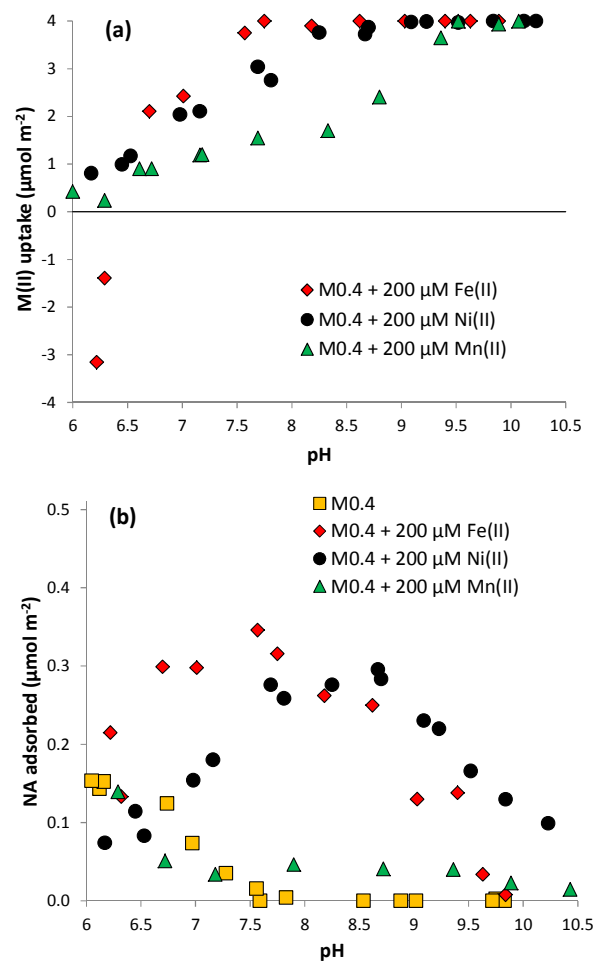
464



465

466

Figure 1



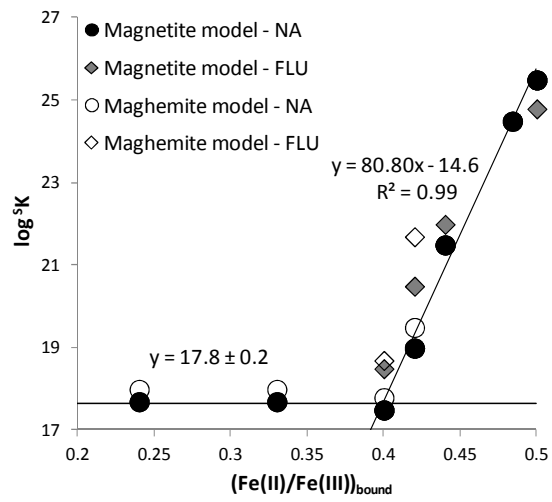
467

468

Figure 2

469

470



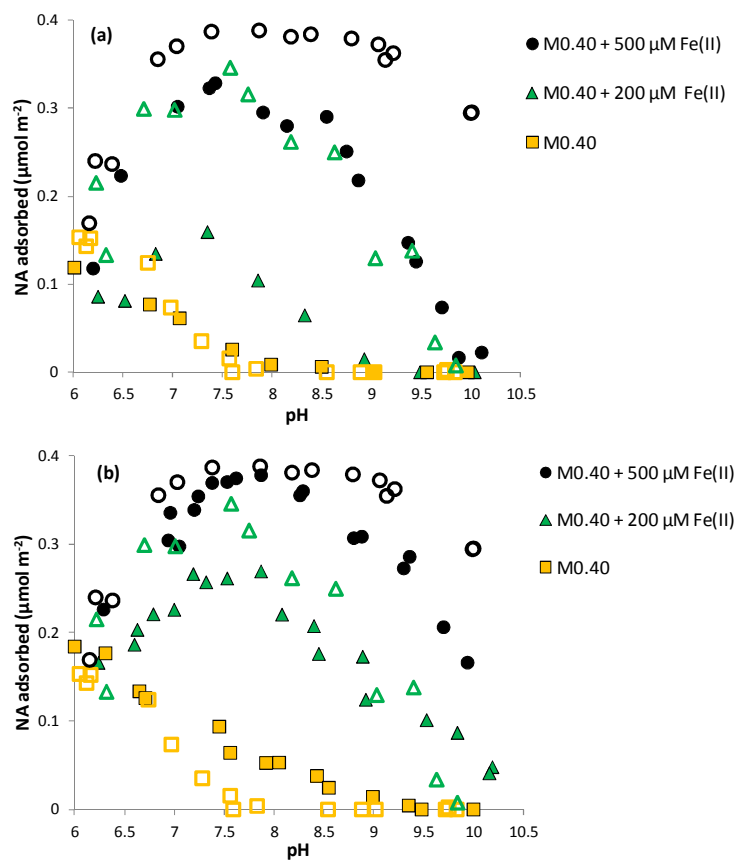
471

472

Figure 3

473

474



475

476

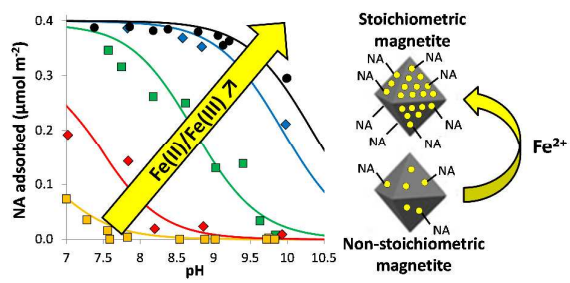
477

Figure 4

478

479

TOC



480

481

482

483